

LA-UR-22-30973

Accepted Manuscript

Los Alamos National Laboratory Double Shell Program Target Development

Schmidt, Derek William; Donovan, Patrick Mark; Edwards, Stephanie Lynn; Fierro, Franklin; Haines, Brian Michael; Hamilton, Christopher Eric; Keiter, Paul Arthur; Loomis, Eric Nicholas; Morrow, Tana; Palaniyappan, Sasikumar; Patterson, Brian M.; Randolph, Randall Blaine; Robey, Harry F. III; Sauppe, Joshua Paul; Stark, David James; Vodnik, Douglas R.

Provided by the author(s) and the Los Alamos National Laboratory (2023-10-18).

To be published in: Fusion Science and Technology

DOI to publisher's version: 10.1080/15361055.2023.2213812

Permalink to record:

<https://permalink.lanl.gov/object/view?what=info:lanl-repo/lareport/LA-UR-22-30973>



Los Alamos National Laboratory, an affirmative action/equal opportunity employer, is operated by Triad National Security, LLC for the National Nuclear Security Administration of U.S. Department of Energy under contract 89233218CNA000001. By approving this article, the publisher recognizes that the U.S. Government retains nonexclusive, royalty-free license to publish or reproduce the published form of this contribution, or to allow others to do so, for U.S. Government purposes. Los Alamos National Laboratory requests that the publisher identify this article as work performed under the auspices of the U.S. Department of Energy. Los Alamos National Laboratory strongly supports academic freedom and a researcher's right to publish; as an institution, however, the Laboratory does not endorse the viewpoint of a publication or guarantee its technical correctness.

Los Alamos National Laboratory Double Shell Program Target

Development

Derek William Schmidt^{a,*}, Patrick Mark Donovan^a, Stephanie Lynn Edwards^a, Franklin Fierro^a, Brian Michael Haines^a, Christopher Eric Hamilton^a, Paul Arthur Keiter^a, Eric Nicholas Loomis^a, Tana Morrow^a, Sasikumar Palaniyappan^a, Brian M. Patterson^a, Randall Blaine Randolph^a, Harry F. Robey^a, Joshua Paul Sauppe^a, David James Stark^a, Douglas R. Vodnik^a

^a*Los Alamos National Laboratory*

SM30 Bikini Atoll Rd., MS E549, Los Alamos, NM 87545

*E-mail: dwschmidt@lanl.gov; ORCID 0000-0002-6969-0973

Total Number of pages: 15 (8 Page including Title pages, 7 pages for figures)

Please print in color.

Comments:

Submission is part of the special issue: 24th Target Specialist Virtual Meeting

Los Alamos National Laboratory Double Shell Program Target Development

Abstract

The Double Shell Program is studying an alternative platform for achieving robust alpha-heating at the National Ignition Facility. Double shells benefit from having a low convergence ratio and lower predicted temperature for achieving volume ignition. The joint required to assemble a double shell is an imperfection in the outer shell that seeds instabilities which can greatly impact the inner capsule's implosion at bang time. Different variations of the shape and placement of the joint were implemented with improvements in the quality of the machining led to measurable improvements in yield. High-z coatings on the outer joint mitigated the impact of the 1-2 micrometer gap sometimes found in double shell assemblies.

Keywords: double; shell; joint

I. Introduction:

Double shell capsules for fusion experiments are an interesting alternative to single shell central hot spot inertial confinement fusion (ICF) concepts due to their benefits of a low-convergence robust burn (Ref. 1,2). This benefit of the deuterium-tritium (D-T) fuel operating in a volume burn regime is that the fuel achieves a more spatially uniform density and temperature profile. The primary double shell program at Los Alamos National Laboratory (LANL) drives the double shell by indirect drive, indirect drive works by placing the double shell capsule inside of a hohlraum driven by the 192 beam National Ignition Facility (NIF) where laser energy is converted to x-ray radiation drive (Ref. 3). Balance of the various laser regions within the Hohlraum control the shape and implosion of the double shell (Ref. 4,5,6).

LANL's double shell point design (Figure 1) uses an outer Al ablator, a low-density CH foam cushion, and an inner shell of W overcoated with a Be tamper layer. The implosion of the double shell is initiated by the ablation of the outer shell's surface creating an opposite force that drives the outer ablator to converge on the inner shell. The kinetic energy is transferred from the outer ablator to the inner shell that encapsulates the D-T fuel. The foam cushion provides a physical back pressure to control the imploding outer shell to evenly implode on the inner shell. The inner shell is tungsten, which helps to trap radiation losses and tamp the expansion of the burning D-T fuel. Beryllium is coated over the tungsten to act as a low-z tamper to reduce expansion of the tungsten from the flux of M-band and L-band X-rays emanating from the hohlraum walls. This low density beryllium tamper also improves the Atwood number (density mismatch) of the low density foam cushion to tungsten interface. Too large of an Atwood number would result in large impacts of Rayleigh-Taylor and Richtmyer-Meshkov instability growth during implosions. We currently use a surrogate deuterated carbon foam (made by General Atomics) to utilize neutron diagnostics for the stagnation conditions before implementing fill lines to deliver the D-T fuel. This paper expands on the previous developments done at LANL (Ref. 7). LANL's double shell program is currently developing studies to measure the impact of the outer shell wall variation, surface finish, and future fill tube impacts to the overall robustness of the design.

II. Outer Ablator Joint Concept Development:

The outer ablator has a joint so that the inner shell and foam cushion can be assembled within and glued together. Any gap in this outer aluminium ablator widens during the implosion and creates a perturbation that imprints onto the inner capsule during the shell collision (Ref. 8). This imprinting onto the inner shell distorts the final burn symmetry of the DT fuel and degrades the yield of the platform. The initial joint design of the outer ablator was for a simple step joint. This joint is designed to have a 0.002 mm inner gap to make sure that the outer surface of the step joint is the surface that seals and bottoms out. White-light interferometer scans of the step joint height all the way around the shell show stresses in the aluminium grain structure that buckle and create variations in the step height around the shell up to 0.001 mm. The internal 0.002 mm gap is designed to consider this variability in the step height so that the outer surface of the joint comes in contact first before the inner surface. This small gap also allows for a volume for the glue to go and bond while the outer surface bottoms out metal to metal. Simulations were done to see if placing the vertical part of the joint would benefit by being closer to the inner part of the capsule or if being more towards the outer region of the ablator could minimize the imprint onto the inner shell (see Figure 2). Simulations showed that moving the vertical component of the step joint farther out improved the final symmetry (Ref. 8). Figure 4a shows the initial placement of the joint in the middle compared to the moving of the joint farther out in Figure 4b.

A second concept was chosen to investigate if a v-groove joint would be a more forgiving geometry that would minimize the impact of the opening on the inner capsule. Simulations were done with the angle of the v-groove at 15°, 30°, and 45° shown in Figure 3. The minimal impact on the inner capsule can be seen in Figure 3b that the 45° joint has the minimal impact on the inner capsule. One set of machined v-groove shells was fielded successfully as shown in Figure 4d. Since glue is used to hold the two outer hemi-shells together, a small 4µm chamfer is cut into the point of the v-groove for a volume for the glue to settle and bond. There is an inner 0.002 mm gap designed into the shell joint to make sure that the outer surface is where the two shells bottom out.

A third hybrid concept was chosen to be an internal flat step joint with an outer slanted joint. This outer slant joint self-centers and levels the two hemi-shells together to help in the alignment of the two shells during robotic assembly. The vertical step joint has radially a 2µm gap for tolerance in the machining to allow the two joints to slide past each other. Internally there is a 0.002 mm gap to compensate for possible

aluminium grain stress variations as well as serve as a volume for the glue to go and bond the two hemi-shells together. In Figure 4e you can see the detail design of the slanted joint design and the CT-scan data in Figure 4f showing a fully closed joint. This slanted joint has become the primary joint design for 2022 and 2023.

The polar region of the hemi-shell, on the inside and outside, is the hardest place to machine and has the largest form and surface finish defects. This is due to the tool coming to a near zero velocity as the tool approaches the center of rotation and starts to rub more than it cuts. The surface finish of this polar region was consistently measured in the range of 1-5 nanometer as shown in Figure 3 from scans from a Zygo White-light Interferometer. Another possible defect in machining shells is having a polar nub from the tool being slightly above or below the axis of the machined shell. A specification that the polar nub from the tool's vertical height had to be less than 400 nanometers. Consistently the pole was machined to be less than 40 nanometers and typically had no measurable nub.

III. Hemi-shell Outer Joint Gold Coating Development:

One concept for preventing the gap in the outer ablator from separating during the radiation drive is to coat the outer area of the joint with a thin gold coating. Stark et al. (Ref. 8) performed simulations that optimized the gold coating to be ideally 75 nanometers on both the male and female outer surfaces of the two halves. Stark showed that the platform was insensitive to the thickness of the gold with minimal impact on yield with variations in the coating thickness of up to 100nm. Typical coating accuracies of a given gold coating are typically within 10nm of target, therefore achieving realistic gold coating to a target thickness to have an impact in improving the mitigation can be counted upon.

Initial thoughts were to use water soluble glue to hold the shell down to the coating fixture to mask the outer surface and glue to hold down an inner machined mask to block the gold coating of the ID and inner step joint. During the removal of the masks, the fixtures were submerged into water but the gold would flake off the extremely smooth diamond-turned aluminium. Adhesion studies were performed to optimized surface preparation for the adhesion of the gold to aluminium, with the optimal process found to be plasma pen cleaning, a strike layer of titanium, and the gold being laid down with E-beam. Even with this optimized adhesion preparation, subsequent gold coatings flaked off during the water submersion to dissolve the glue.

A mechanical trap fixture was designed with a precision machined plastic mandrel to mask the internal surfaces of the joint, and a precision machined 3D printed plastic fixture to hold and mask the outer surface. The internal mask was machined out of Delrin to be a high temperature resistant plastic. The outer masking fixture was printed from Microfine Grey from Protolabs. A vacuum channel was designed to go to each hemi-shell to hold the shell down during assembly. The pocket for each shell was machined on a precision mill to make sure the outer diameter and profile of the pocket was exact. Each arm of the mechanical fixture is spring loaded and set screw driven to lower each arm of the fixture down to trap each shell and inner surface mask (Figure 6a). Gold coatings successfully adhered to the outer surface and was measured to have roughly the same surface finish of the pre-coated surface at <10 nanometers. Some shadowing was seen on the initial coating test from the six arms as they come out from the center of the fixture. To minimize and even out any shadowing, the coating fixture was tilted so slightly in one direction and the coating thickness was divided into four different coating runs with the coating fixture rotated 90° in between subsequent coating runs.

IV. Assembly Development:

Previous assembly of LANL Double Shells were glued together using small micro-dots of glue on a fiber that were placed by hand or by robotic arm (Ref. 7). New glue dispensing hardware, Nordson Ultimius V, was mounted onto the robotic arm (Ref. 9) to dispense micro-dots of glue inside the inner radius of the step joint. Two micro-dots of glue were placed 180 degrees apart using 0.080 mm inner diameter tips. Low viscosity Norland 68 glue was used because, due to its low viscosity, it wicks easily into the inner gap and cures better under light tight gaps with the UV-cure lights.

Initially the seams of the foam hemi-shells were assembled in line with the joint on the equator. Starting in March 2022 through September 2022 all foam assemblies were assembled with the foam seam vertical and orthogonal to the equator in the outer ablator shells (See Figure 7). This was done to move a possible perturbation from the foam seam away from the known perturbation of the outer ablator joint. Two individual vacuum chucks for the foams were designed and 3D printed with web support structures to support and hold the shell. After the two foams and inner capsule were assembled, a third vacuum chuck would come in on the robot and pick up the assembly to rotate it and insert it into the lower shell for final assembly.

V. Summary:

The Double Shell Program at LANL has been studying the various impacts of outer shell joint closure, internal surface finish, and polar nub features on the impact of those defects to the robustness of the platform for robust burn. Currently simulations and studies are still underway to fully take into effect all the various impacts and how they will degrade the yield and vary the robustness of the platform. LANL has been exploring new joint concepts to minimize the impact of any opening in the joint to the inner capsule through different variations in the joint geometry. All these new concepts were successfully machined, assembled, and fielded on NIF resulting in increased yields with improvements in the joint profile and minimization to the joint gap. Physicists through modelling have shown that a gold coated joint at the correct thickness will drastically minimize the separation of any gap in the joint during the drive of the outer ablator. A new mechanical coating fixture was designed to eliminate the use of any water-soluble glue that would require submersion in water. Improvements on that fixture included spring loaded arms that could be independently lowered to apply a constant holding force for each shell. Gold coatings were successfully coated onto two runs showing the future viability of the approach to solve imperfections in the outer aluminium ablator shell. Lastly a new approach was developed to assemble the two foam halves and internal capsule together and rotate so that the foam mating seam would be orthogonal to the ablator joint.

References:

1. O.A. Hurricane et al., "Fuel gain exceeding unity in an inertially confined fusion implosion," *Nature* **506**, 13008 (2014)
2. H. Abu-Shawareb et al., "Lawson Criterion for Ignition Exceeded in an Inertial Fusion Experiment," *Physics Review Letters* **129**, 075001 (2022)
3. E.C. Merritt et al., "Experimental Study of Energy Transfer in Double Shell Implosions," *Physics of Plasmas* **26**, 052702 (2019)
4. D. Montgomery et al., "Design Considerations for Indirectly Driven Double Shell Capsules," *Physics of Plasmas* **25**, 092706 (2018)
5. E.N. Loomis, "Mechanisms of Shape Transfer and Preheating in Indirect-drive Double Shell Collisions," *Physics of Plasmas* **29**, 062704 (2033)
6. P. Amendt, "Indirect-drive Noncryogenic Double-shell Ignition Targets for the National Ignition Facility: Design and Analysis," *Physics of Plasmas* **9**, 2221 (2002)
7. T. Cardenas et al., "Progress Toward Fabrication of Machined Metal Shells for the First Double-Shell Implosions at the National Ignition Facility," *Fusion Science and Technology* **73**, (2018)
8. D.J. Stark et al., "Detrimental Effects and Mitigation of the Joint Feature in Double Shell Implosion Simulations," *Physics of Plasmas* **28**, 052703 (2021)
9. D.W. SCHMIDT, "Development of the Triple Theta Assembly Station with Machine Vision Feedback," *Fusion Sci. Technol.*, **55**, 3, 290 (2009)

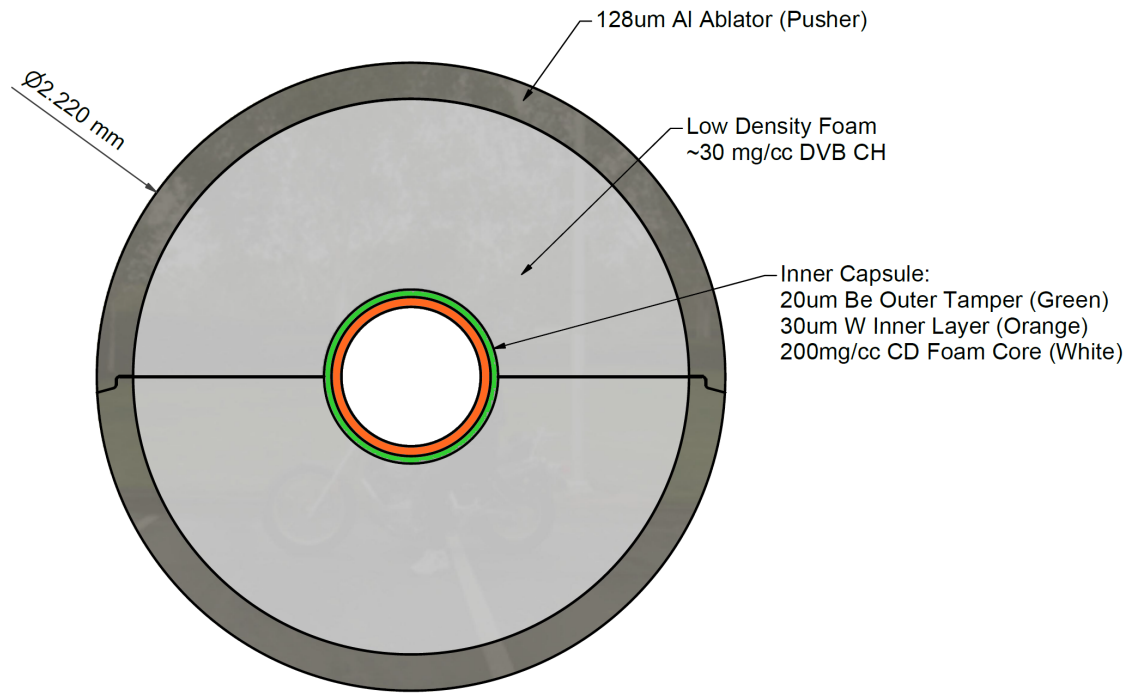


Figure 1, Double Shell basic concept and point design.

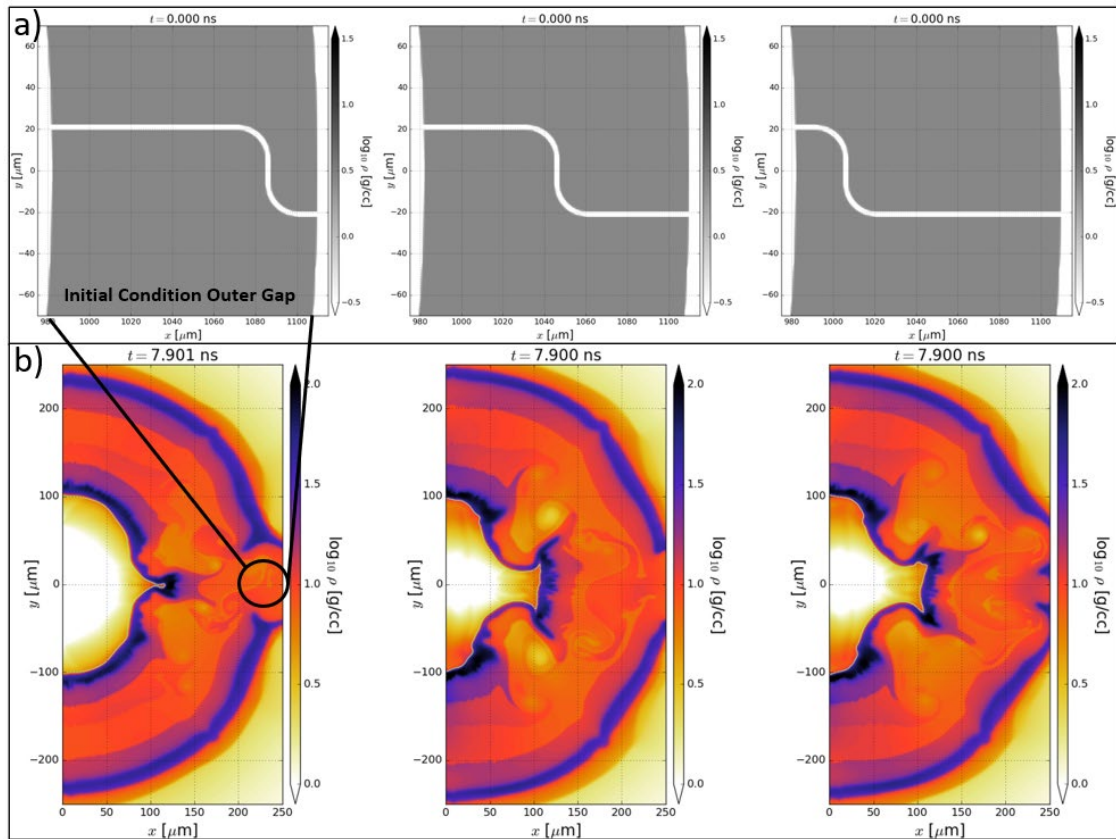


Figure 2, a) Initial conditions of simulations setting the placement of the joint in the shell from the outer surface on the left to the inner surface on the right. b) simulations illustrating varying impact of the outer ablator joint on the inner capsule.

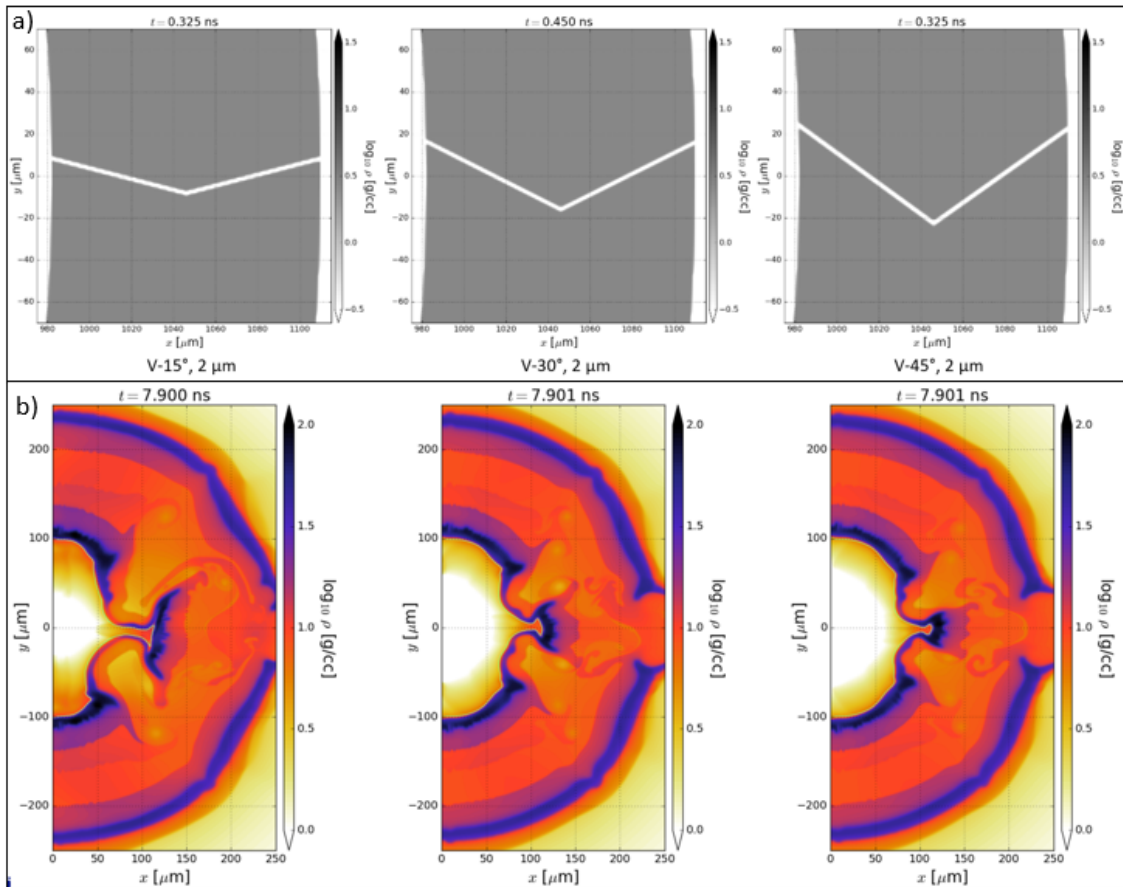


Figure 3, a) Initial conditions v-groove at 15 degree on the left to 45 degrees on the right, b) corresponding simulations at $t=7.9$ ns of the impact of the outer ablator joint on the inner capsule

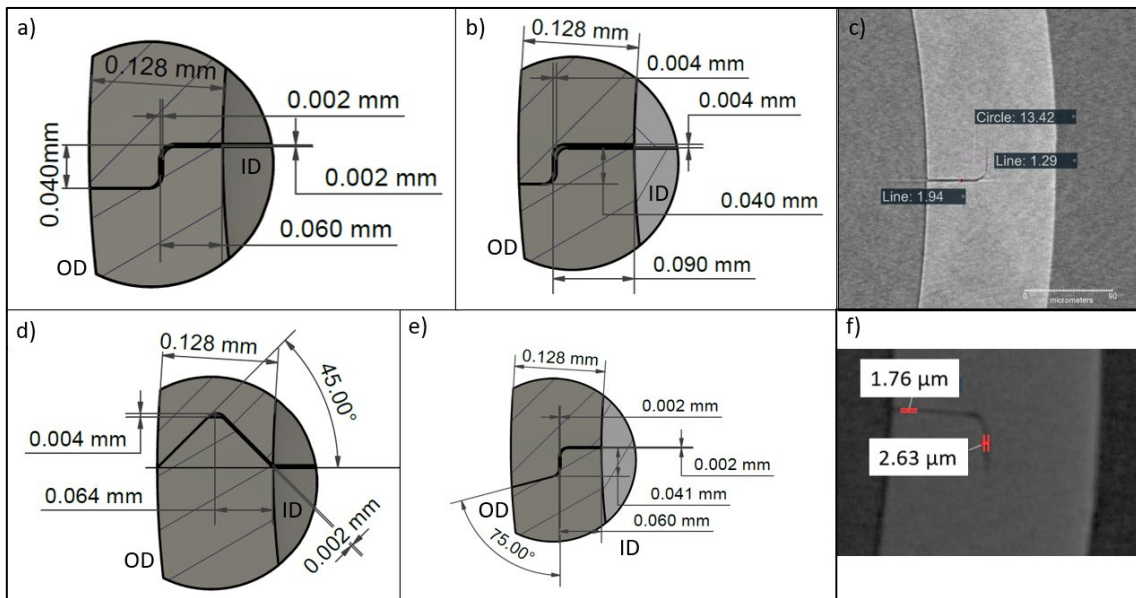


Figure 4, a) Design with simple step in middle (Sept. 2021), b) joint moved closer to outside wall (Nov. 2021), c) successful assembly of middle step joint, d) V-groove design (March 2022), e) slanted joint design (Aug. 2022), f) successful assembly of slanted joint

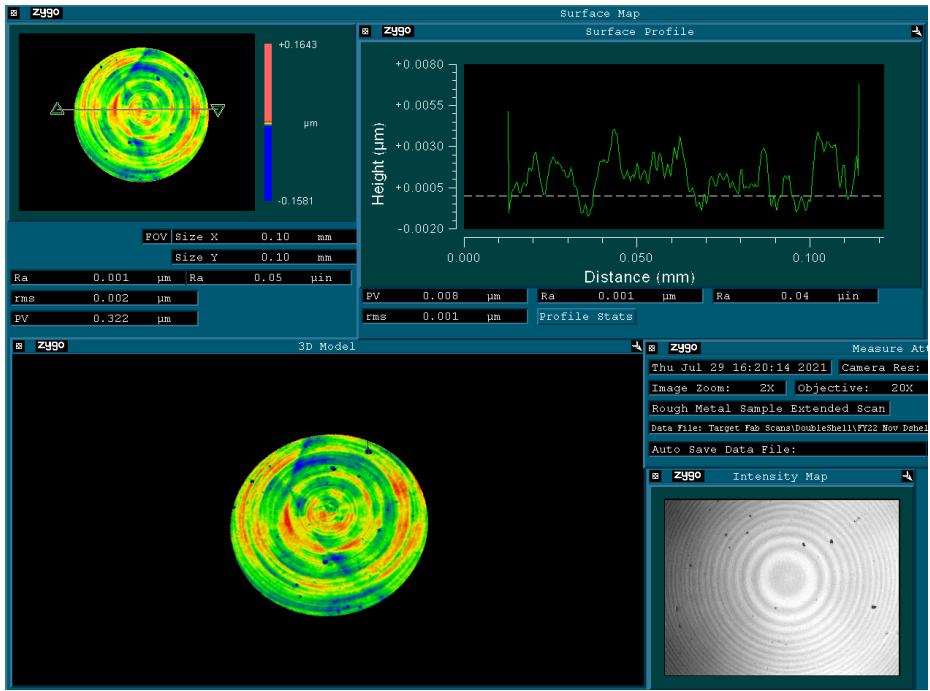


Figure 5, White-light interferometer scans of a pole on an OD of a shell showing 1 nanometer surface finish and no-measurable nub from a tool height offset

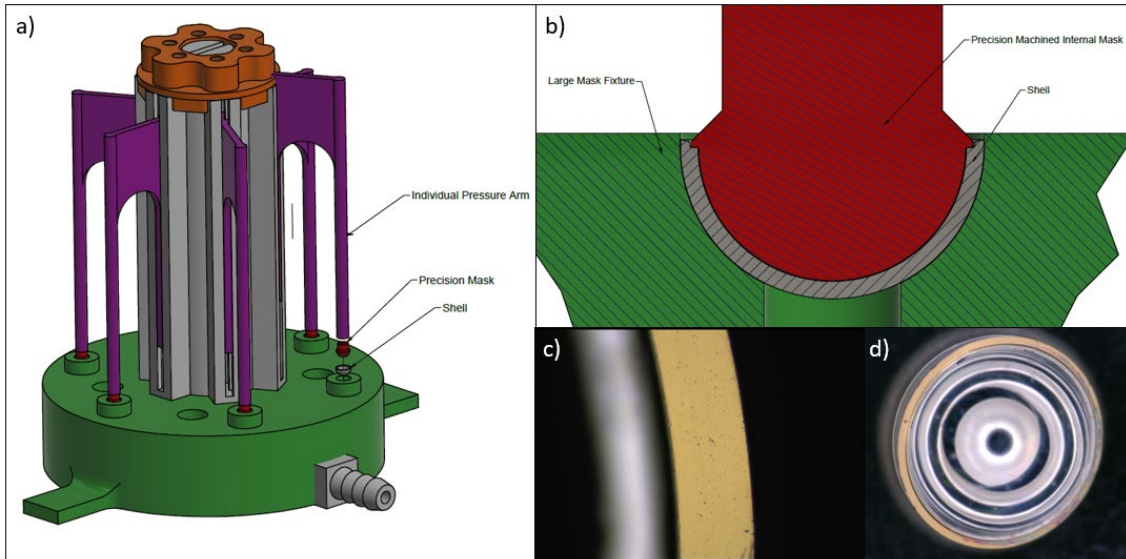


Figure 6, a) Mechanical trapping fixture with individual arm control, b) Detail view of fixture and mask, c) High-mag view of gold coating, d) Overall view of gold coated slant joint

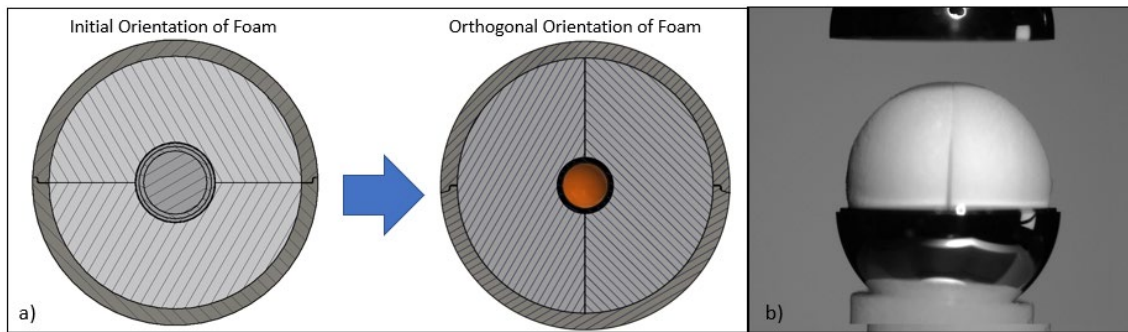


Figure 7, a) Original orientation compared to an orthogonal orientation, b) First orthogonal foams in March 2022